

Thin-skin eddy-current inversion for the determination of crack shapes

J R Bowler

Iowa State University, Center for Nondestructive Evaluation, Applied Sciences Complex II,
1915 Scholl Road, Ames, IA, USA

E-mail: jbowler@cnde.iastate.edu

Received 24 May 2002

Published 8 November 2002

Online at stacks.iop.org/IP/18/1891

Abstract

An important aim of nondestructive evaluation is to quantify flaws in components using sensor measurements. In pursuit of this aim, a method has been developed for finding the size and shape of planar cracks in electrical conductors from single-frequency eddy-current probe impedance measurements. In the direct problem, the change in the impedance of an eddy-current probe due to a crack in a conductor is determined in the regime where the skin depth is much smaller than the dimensions of the crack face. The thin-skin field at the crack face is represented by a potential satisfying the two-dimensional Laplace equation. In the corresponding inverse problem, the crack shape is sought from probe impedance measurements. Here the crack boundary is located using an iterative inversion scheme in which a cost function quantifying the overall difference between predictions and measurements is minimized using a gradient method. The gradient is found from the derivative of the cost function with respect to a variation of the flaw. Shape estimates found by the inversion of impedance data have been compared with the measured profiles of simulated cracks in aluminium plates. The comparisons show that the inversion scheme gives good agreement with direct physical measurements.

1. Introduction

Eddy-current nondestructive inspection uses inductive probes to excite currents in metallic components and to sense the presence of defects through changes of probe impedance [1]. Calculations of the probe response can neglect displacement current because of the overwhelming dominance of charge conduction. The quasi-static field in the conductor migrates in accordance with a vector diffusion equation. For a time-harmonic excitation, the ‘wavenumber’ is complex having equal real and imaginary parts. An electromagnetic disturbance therefore attenuates rapidly with distance from the surface of the conductor on a scale determined by the skin effect.

In creating a theoretical framework for direct and inverse problems, flaws can be defined in terms of the boundary at which the electrical conductivity and magnetic permeability changes. By using inversion techniques, the shape and size of flaws are sought from probe measurements. An ideal crack is represented theoretically as an impenetrable barrier to electric current and the quasi-static electromagnetic field is calculated to predict the probe impedance variation with position for comparison with the measurements. Here, the crack shape is sought through a standard iterative inversion scheme in which a cost function quantifying the overall difference between predictions and measurements is minimized using a conjugate gradient method. Despite the intrinsic non-linearity of the problem, false minima have not given rise to difficulties.

It is assumed that the crack lies in a known plane perpendicular to the surface of the conductor and has negligible or known opening. The inverse problem then reduces to one of finding a function that defines the line of the crack edge. The required functional derivative of the cost function is determined from the corresponding derivative of the probe impedance with respect to a variation of this line. The latter has been derived in a previous inversion study for an ideal crack excited at an arbitrary frequency [2, 3]. Here, the impedance derivative is determined for the case where the skin depth is small in comparison with the dimensions of the crack face. For a thin-skin excitation, the current density decays exponentially with the perpendicular distance from the crack surface. Its distribution on the crack face is governed by a potential satisfying the two-dimensional Laplace equation with distinct boundary conditions at the crack edge and the crack mouth. Hence the direct problem is solved by finding a harmonic function whose domain corresponds to the face of the crack.

The approach taken in this paper evolved from the pioneering work of Kahn *et al* [4] who considered a two-dimensional thin-skin surface crack problem. Assuming that the skin depth is small compared with the crack depth, the field at the edge decouples from the solution at the crack mouth. The edge solution can then be adapted from Sommerfeld's half-plane diffraction theory [5] by substituting a complex wavenumber for a real one. The impedance associated with the long straight crack in a field invariant along its length has been calculated by integrating the Poynting vector over the crack surface to give a simple analytical result [6]. The small skin depth approximation has also been applied to finite-length crack problems [7] and used to treat a simple inverse problem for a long crack of constant depth excited by a non-uniform field [8].

2. Direct problem formulation

2.1. Transverse magnetic potential

In this work, thin-skin approximations are used for forward and inverse finite-crack problems. In the configuration considered, eddy currents are induced by a circular coil whose axis is normal to the plane surface of a conductor containing an ideal crack, figure 1. The crack plane is perpendicular to the surface of a half-space conductor. The ideal crack has negligible opening yet is impenetrable to electric current. In the forward problem the aim is to calculate the field at the crack faces and, from the solution, determine the coil impedance change due to the flaw. A brief description of the problem formulation is presented below summarizing a more detailed account given elsewhere [9, 10]. Later in this paper it will be necessary to consider the effects of a finite opening since this has a significant effect on the probe impedance variation due to slots, but initially the opening is neglected.

The field in the conductor is expressed in terms of Hertz potentials representing transverse electric (TE) and transverse magnetic (TM) modes defined with respect to a preferred direction

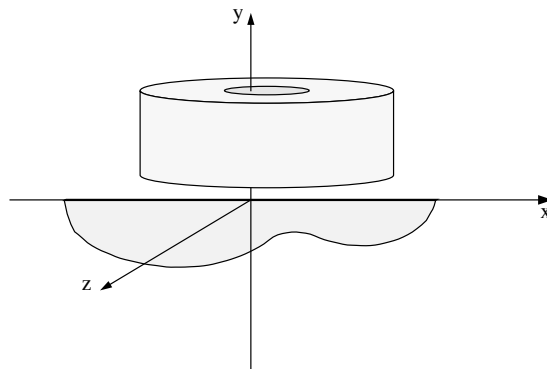


Figure 1. A normal coil over a surface-breaking crack in a conductor.

normal to the crack face. With a negligible crack opening, no direct TE interaction with the ideal crack occurs but because the preferred direction is *parallel to the material interface*, the modes are coupled at the surface plane leading to indirect perturbation of the TE mode via the TM mode. However, the primary electromagnetic interaction with the ideal crack is through the TM mode.

Let the normal to the crack face be in the z -direction and express the magnetic field of the TM mode in the conductor as

$$\mathbf{H} = \nabla \times [\hat{z}\psi], \quad (1)$$

\hat{z} being a unit vector. From Ampère's law, the curl of the magnetic field is equal to the current density \mathbf{J} , therefore

$$\mathbf{J} = \nabla \times \nabla \times [\hat{z}\psi]. \quad (2)$$

Putting $\hat{z} \cdot \mathbf{J} = 0$ for points at the surface of the crack shows that the TM potential satisfies a two-dimensional Laplace equation in a domain corresponding to a crack face. Thus, at arbitrary frequency and skin depth,

$$\left(\frac{\partial^2}{\partial x^2} + \frac{\partial^2}{\partial y^2} \right) \psi(x, y) = 0. \quad (3)$$

The domain of equation (3) is bounded by a line corresponding to the crack edge, C_e , and the line of the crack mouth, C_m . In order to find the thin-skin boundary conditions at C_e and C_m for the two-dimensional Laplace problem, it is helpful to outline first the arbitrary-frequency ideal crack problem as follows. At an arbitrary frequency the TM potential due to the ideal crack can be expressed in integral form as a double-layer potential. By approximating this integral form for the double-layer potential in the thin-skin regime, the boundary condition on C_m for the Laplace problem is found.

2.2. Double-layer potential

Let an ideal crack in an induced electric current stream be defined on an open surface S_0 . The current density is given in terms of a TM potential by (2) and the potential is a solution of the Helmholtz equation

$$(\nabla^2 + k^2)\psi = 0, \quad (4)$$

where $k^2 = i\omega\mu_0\mu_r\sigma_0$, μ_r being the relative permeability and σ_0 the conductivity of the host conductor. While the tangential magnetic field is continuous at S_0 , the tangential electric field

and indeed the electric current density are discontinuous. From (1), it can be seen that by making ψ continuous at S_0 , the continuity of the tangential magnetic field is secured. The discontinuity of the tangential current density together with (2) shows that the normal gradient of ψ is discontinuous. Thus ψ is a double-layer potential that can be expressed using an integral formula as

$$\psi(\mathbf{r}) = \psi^{(0)}(\mathbf{r}) - \int_{S_0} G(\mathbf{r}, \mathbf{r}') \left[\frac{\partial \psi}{\partial z'} \Big|_+ - \frac{\partial \psi}{\partial z'} \Big|_- \right] dS' \quad (5)$$

where the + and - subscripts indicate points at the approach to the positive and negative crack faces respectively. $\psi^{(0)}(\mathbf{r})$ represents the unperturbed potential. The Green function for the TM potential in a half-space conductor, $G(\mathbf{r}, \mathbf{r}')$, has been derived taking into account that the preferred direction is parallel to the surface of the conductor. With this choice, a singular TM source in the conductor gives rise to a TM field and a TE field due to mode coupling at the interface. Similarly, a TE source gives rise to both modes. Commonly, mode coupling is avoided by choosing the preferred direction normal to the interface but here the main concern is to avoid mode coupling at the crack plane. With this non-standard choice of reference direction, the TM half-space Green function is [9]

$$G(\mathbf{r}, \mathbf{r}') = \frac{e^{ik|\mathbf{r}-\mathbf{r}'|}}{4\pi|\mathbf{r}-\mathbf{r}'|} + \frac{e^{ik|\mathbf{r}-\mathbf{r}''|}}{4\pi|\mathbf{r}-\mathbf{r}''|} + \frac{\partial^2}{\partial x^2} U(x-x', y+y', z-z'), \quad (6)$$

where $\mathbf{r}'' = \mathbf{r}' - 2\hat{y}y'$ is the image point and

$$U(x, y, z) = \frac{\mu_r k^2}{(2\pi)^2} \int_{-\infty}^{\infty} \int_{-\infty}^{\infty} \frac{1}{v^2 - k^2} \left(\frac{1}{\kappa} - \frac{\mu_r}{\gamma} \right) \frac{1}{[(\mu_r^2 - 1)\kappa^2 + k^2]} e^{\gamma y + iux + ivz} du dv, \quad (7)$$

with $\gamma = (u^2 + v^2 - k^2)^{1/2}$ and $\kappa = (u^2 + v^2)^{1/2}$, taking roots with positive real parts.

2.3. Boundary conditions

The boundary conditions on ψ for the surface Laplace problem have been derived assuming that the skin depth is much smaller than the length and depth of the crack. At the buried edge of the crack, the thin-skin magnetic field normal to the edge in the crack plane is zero [7, 8]. This condition is satisfied by requiring that the TM potential at the edge is constant. Putting the constant to zero gives the edge boundary condition

$$\psi(x, y) = 0 \quad \{x, y\} \in C_e. \quad (8)$$

In the thin-skin regime, the potential near the crack plane varies as $e^{ik|z|}$, therefore one may approximate the jump in the potential gradient at the crack as

$$\frac{\partial \psi}{\partial z} \Big|_+ - \frac{\partial \psi}{\partial z} \Big|_- \approx 2ik\psi_{\pm}. \quad (9)$$

Differentiating (5) with respect to y , using (9) and considering a field point at the crack mouth gives

$$f(x) = \frac{\partial \psi(x, y)}{\partial y} \Big|_{y=0} + \int_{C_m} K(x-x') \psi(x', 0) dx', \quad \{x, y\} \in C_m, \quad (10)$$

where the integral is taken along the line of the crack mouth and $f(x) = \partial \psi^{(0)}/\partial y$ is the x -component of the unperturbed magnetic field on C_m . The kernel $K(x-x')$ is given by

$$K(x) = 2ik \frac{\partial^2}{\partial x^2} U(x, 0, 0). \quad (11)$$

In deriving (10) from (5), the integration over y' is carried out assuming the function $\psi(x', y')$ is approximately constant over the limited depth range of the integral kernel in the thin-skin limit.

The boundary condition, equation (10), expresses the x -component of the unperturbed magnetic field at the mouth of the crack as the total minus the perturbed field. In the work of others [7, 8], the mouth boundary condition was approximated by neglecting the effect of the perturbed field at C_m . Although this omission simplifies the calculations, predictions made without the integral term are less accurate than those which include it [9].

3. Solution of the direct problem

3.1. Approach

A solution of equation (3) is sought for cracks of smooth shape by using a general conformal mapping which transforms a complex-plane representation of the crack face region into a rectangular domain. In the case of a semi-elliptical crack, as well as for all the other shapes considered, the crack mouth is divided into three segments by two foci. Each of the three segments is then mapped to one side of a rectangle and the crack edge maps to the fourth side. The Laplace equation for a potential defined on a rectangular domain is readily solved.

A suitable mapping has been found for a general class of crack shapes but it is difficult to apply the integral boundary condition, equation (10), on three sides of the transformed domain. This complication is avoided by using an approximation as follows. The solution is first expressed as

$$\psi = \psi_1 + \psi_2, \quad (12)$$

where ψ_1 satisfies the Laplace equation in a rectangular region whose length, $2a$, and depth, b , is equal to the overall length and depth of the crack. The function ψ_2 is a solution defined in the actual crack domain whether this be semi-elliptical or some other shape. The solution ψ_1 is found exactly as for a rectangular crack which means it vanishes on three sides of the boundary:

$$\psi_1 = 0, \quad \begin{cases} x = \pm a, & 0 \leq x \leq b, \\ -a < x < a, & y = b, \end{cases} \quad (13)$$

and at the mouth satisfies

$$f(x) = \left. \frac{\partial \psi_1(x, y)}{\partial y} \right|_{y=0} + \int_{C_m} K(x - x') \psi_1(x', 0) dx'. \quad (14)$$

The first part of the solution of (3) is expressed in the form

$$\psi_1(x, y) = \sum_n D_n \frac{2a \sin[(n\pi/2)(x/a + 1)] \sinh[(n\pi/2)(b - y)/a]}{n\pi \cosh(n\pi b/2a)}, \quad (15)$$

which satisfies (13). Substituting into (14), multiplying by $\sin[(m\pi/2)(x/a + 1)]$ and integrating between $-a$ and a gives a matrix equation which is solved numerically to give the expansion coefficients, D_n .

The potential ψ_2 satisfies

$$\left. \frac{\partial \psi_2(x, y)}{\partial y} \right|_{y=0} = 0 \quad \{x, y\} \in C_m, \quad (16)$$

at the crack mouth. At the crack edge

$$\psi_2(x, y) = G(x, y), \quad \{x, y\} \in C_e. \quad (17)$$

In order to comply with (8), the function $G(x, y)$ is defined by letting

$$G(x, y) = -\psi_1(x, y), \quad \{x, y\} \in C_e. \quad (18)$$

It can be seen from (14) and (16) that (10) is not satisfied exactly but is approximated by neglecting ψ_2 in the integral. Because ψ_2 is small compared with ψ_1 and the integral term is itself relatively small, the approximation is reasonable as can be corroborated from the comparison of direct problem predictions with experiment [11].

3.2. General mapping

A mapping of the form

$$\zeta = x + iy = \sum_v K_v \cos[v\pi(1 - \tau)], \quad (19)$$

where $\tau = \xi + i\eta$ and $v = 1, 2, \dots, N$, transforms the representation of the crack domain in the complex ζ -plane into a rectangular region in the τ -plane. Parametric equations for the line of the crack edge are found by putting $\eta = \alpha$ in (19), where α is a real constant. Equating real and imaginary parts gives

$$x = \sum_v a_v \cos[v\pi(1 - \xi)] \quad (20)$$

$$y = \sum_v b_v \sin[v\pi(1 - \xi)] \quad (21)$$

where

$$a_v = K_v \cosh(v\pi\alpha) \quad (22)$$

and

$$b_v = K_v \sinh(v\pi\alpha). \quad (23)$$

In the direct problem, the parameters are chosen to give a good representation of a given flaw shape by a least-squares fitting procedure. For a semi-elliptical crack only one term is needed in the summation, equation (19). In general, three or four terms give a good approximation of a smooth crack shape using what we refer to as an elliptical epi-cycloidal representation [11]. In the inverse problem, the coordinate x_0 of the mid-point of the foci, the parameter α and the coefficients K_v are sought from observations of impedance.

Now the second part of the solution, ψ_2 , is written as

$$\psi_2(x, y) = \phi[\xi(x, y), \eta(x, y)], \quad (24)$$

where

$$\phi(\xi, \eta) = \sum_n C_n \frac{\cos(n\pi\xi) \cosh(n\pi\eta)}{\cosh(n\pi\alpha)}. \quad (25)$$

In the τ -plane, the boundary condition (16) becomes

$$\frac{\partial\phi}{\partial\xi} = 0, \quad \xi = 0 \text{ or } 1, \quad 0 \leq \eta \leq \alpha, \quad (26)$$

$$\frac{\partial\phi}{\partial\eta} = 0, \quad 0 \leq \xi \leq 1, \quad \eta = \alpha, \quad (27)$$

and (8) is satisfied by putting

$$\phi(\xi, \alpha) = g(\xi), \quad 0 \leq \xi \leq 1, \quad (28)$$

where $g(\xi)$ is given by mapping the function $G(x, y), \{x, y\} \in C_e$ into the τ -plane. Clearly (25) satisfies (26) and (27). The expansion coefficients in (25) are found from

$$C_m = 2 \int_0^1 g(\xi) \cos(m\pi\xi) d\xi \quad (29)$$

which is derived using the orthogonal properties of the cosine function. This completes the summary of the solution of the direct problem. Next the calculation of the observed probe impedance is considered.

3.3. Impedance

The impedance change of a coil due to the presence of a crack can be calculated from an expression derived using a reciprocity theorem. Taking into account a correction for the crack opening, the impedance change due to a crack is given by [10]

$$Z = \beta \int_C \psi(x, 0) f(x) dx, \quad (30)$$

where

$$\beta = -\frac{k}{\sigma I^2} \left(kc \frac{\mu_c}{\mu_r} + 2i \right). \quad (31)$$

Here c is the crack opening, I is the probe current and μ_c is the relative permeability of the material within the crack volume. For a probe consisting of a normal coil of rectangular cross section, the incident field, $f(x)$, can be calculated using a closed-form expression [12].

The crack opening has been introduced here because it gives rise to a term that is of leading order with respect to its k dependence. Even if the opening c is so small that it has a negligible effect on the field at the crack face, the crack opening gives rise to the dominant contribution to the impedance in the high-frequency limit and must be included. Other terms associated with the crack opening which involve integration of the field over the area of the crack mouth and edge have been omitted from equation (30). Additional small terms omitted from equation (30) but included in the forward predictions account for the fact that the flow of electric current near the crack mouth and edge is not parallel to the crack face [9]. By neglecting these additional contributions in the inverse problem, minor errors arise in computing the impedance gradient. These may marginally slow the rate of convergence but, by using (30) rather than the full expression, the computational cost of computing the effects of minor terms is avoided.

4. Crack profile inversion

4.1. Least-squares optimization

Let the crack shape be defined in terms of a flaw function $v(\mathbf{p}, x, y) = 0$ representing the equation of the line of the crack edge. The flaw function depends on n parameters $p_1, p_2, p_3, \dots, p_n$, collectively denoted by the vector \mathbf{p} . These parameters are sought by minimizing a cost function using a gradient method. The cost function, otherwise known as an error or penalty function, is a measure of the overall difference between predictions and observations. Summing over all observations, the cost function is defined by

$$\mathcal{E}(\mathbf{p}) = \sum_{m=1, M} |Z_m(\mathbf{p}) - Z_m^{\text{obs}}|^2, \quad (32)$$

where Z_m^{obs} is the observed contribution to the impedance of an eddy current probe at the m th observation point due to a crack and $Z_m(\mathbf{p})$ is the corresponding prediction.

In order to find the set of flaw parameters that minimize the cost function, the derivative with respect to each parameter is calculated. From (32), the partial derivative with respect to parameter p_j is given by

$$\frac{\partial \mathcal{E}}{\partial p_j} = 2 \operatorname{Re} \left\{ \sum_{m=1, M} [Z_m(\mathbf{p}) - Z_m^{\text{obs}}]^* \frac{\partial Z(\mathbf{p})}{\partial p_j} \right\}, \quad (33)$$

where Re denotes the real part and $*$ denotes the complex conjugate. The derivatives will be found from the functional gradient of the impedance with respect to a variation in the flaw function, v , written as $\nabla_v Z(l)$. The latter can be interpreted as the sensitivity of the probe impedance to a variation in the flaw function at a point on the edge of the crack whose coordinate is l . This function is defined such that an incremental change in the impedance due to an arbitrary variation of the flaw is expressed in the form

$$\delta Z = \int_{C_e} \nabla_v Z(l) \delta n(l) dl, \quad (34)$$

where $\delta n(l)$ represents a displacement of the crack edge in the direction of its normal in the plane of the crack. The function $\nabla_v Z(l)$ is identified in the next section. From (34), the partial derivatives of the impedance are given by

$$\frac{\partial Z}{\partial p_j} = \int_{C_e} \nabla_v Z(l) \frac{\partial n}{\partial p_j} dl. \quad (35)$$

Combining the partial derivatives into the parameter-space gradient vectors $\nabla_p \mathcal{E}$ and $\nabla_p Z$, equation (33) can be written as

$$\nabla_p \mathcal{E} = 2 \operatorname{Re} \left\{ \sum_{m=1, M} [Z_m(\mathbf{p}) - Z_m^{\text{obs}}]^* \nabla_p Z \right\}. \quad (36)$$

Starting with an initial parameter set, denoted by the vector \mathbf{p}_0 , the first update uses a steepest descent step, written

$$\mathbf{p}_1 = \mathbf{p}_0 - \alpha \nabla_p \mathcal{E}, \quad (37)$$

where the step size parameter α is chosen to minimize \mathcal{E} in the direction of its gradient. Thereafter a conjugate-gradient update is used.

Thus the search for a minimum error takes place in a parameter space using the cost function gradient vector $\nabla_p \mathcal{E}$ to determine the search direction and update the flaw parameters. The cost function gradient vector is calculated from the functional gradient of the impedance, $\nabla_v Z(l)$, using equations (35) and (36). We next consider how $\nabla_v Z(l)$ is determined from solutions of the forward problem.

5. Impedance gradient

5.1. Potential variation

In order to determine a general incremental change of probe impedance due to a flaw variation, and thereby identify $\nabla_v Z(l)$, it is necessary to consider how the potential ψ changes as the position of the crack edge is varied. An incremental variation in the position of the line of the crack edge results in a variation $\delta\psi$ in the potential. Thus, following an incremental flaw variation, equation (10) becomes

$$f(x) = \frac{\partial(\psi + \delta\psi)}{\partial y} \Big|_{y=0} + \int_{C_m + \delta C_m} K(x - x') [\psi(x', 0) + \delta\psi(x', 0)] dx', \quad (38)$$

$\{x, y\} \in C_m + \delta C_m.$

The potential ψ is deemed to be zero in the region outside the original crack domain. Subtracting equation (10) from (38) and considering the resulting relationship for the original line of the crack mouth we have

$$0 = \frac{\partial \delta \psi}{\partial y} \Big|_{y=0} + \int_{C_m + \delta C_m} K(x - x') \delta \psi(x', 0) dx', \quad \{x, y\} \in C_m. \quad (39)$$

Equations (38) and (39) are used to derive a simple expression for the impedance variation as follows.

5.2. Impedance variation

From equation (30), the variation of impedance due to an incremental change in the crack profile is given by

$$\delta Z = \beta \int_{C_m + \delta C_m} \delta \psi(x, 0) f(x) dx. \quad (40)$$

Substituting for $f(x)$ from (38) gives

$$\delta Z = \beta \int_{C_m + \delta C_m} \left[\delta \psi \frac{\partial(\psi + \delta \psi)}{\partial y} \Big|_{y=0} + (\psi + \delta \psi) \int_{C_m + \delta C_m} K(x - x') \delta \psi(x', 0) dx' \right] dx,$$

where the order of the integration has been reversed in the double-integral term, variable names x and x' exchanged and the fact that $K(x) = K(-x)$ has been used. The above relationship can also be written as

$$\begin{aligned} \delta Z = & \beta \int_{C_m + \delta C_m} \delta \psi \frac{\partial(\psi + \delta \psi)}{\partial y} \Big|_{y=0} dx + \beta \int_{C_m} (\psi + \delta \psi) \int_{C_m + \delta C_m} K(x - x') \delta \psi(x', 0) dx' dx \\ & + \beta \int_{\delta C_m} \delta \psi \int_{C_m + \delta C_m} K(x - x') \delta \psi(x', 0) dx' dx. \end{aligned}$$

Equation (39), whose field domain is C_m , is used with the second integral above to give

$$\begin{aligned} \delta Z = & \beta \int_{C_m + \delta C_m} \left[\delta \psi \frac{\partial(\psi + \delta \psi)}{\partial y} \Big|_{y=0} - (\psi + \delta \psi) \frac{\partial \delta \psi}{\partial y} \Big|_{y=0} \right] dx \\ & + \beta \int_{\delta C_m} \delta \psi \left[\frac{\partial \delta \psi}{\partial y} \Big|_{y=0} + \int_{C_m + \delta C_m} K(x - x') \delta \psi(x', 0) dx' \right] dx. \end{aligned} \quad (41)$$

Note that the integral over δC_m , being second order in the variation, is negligible. Because both $\delta \psi$ and $\psi + \delta \psi$ are zero at the varied crack edge in accordance with the boundary condition (8), the path of the first integral may be extended to enclose the varied crack. Let C_0 be the clockwise closed path round the original flaw and $C_0 + \delta C_0$ be the path round the varied crack domain, figure 2. Then

$$\delta Z = \beta \oint_{C_0 + \delta C_0} \left[\delta \psi \frac{\partial(\psi + \delta \psi)}{\partial n} - (\psi + \delta \psi) \frac{\partial \delta \psi}{\partial n} \right] dl. \quad (42)$$

This line integral can be expressed as the sum of two closed contour integrals, one following the boundary of the original crack domain C_0 , figure 2(a), and the other following the boundary of the crack extension δC_0 , figure 2(b). It can be shown, using Gauss' theorem, that

$$\int_{S_0} [\psi_1 \nabla^2 \psi_2 - \psi_2 \nabla^2 \psi_1] dS = \oint_C \left[\psi_1 \frac{\partial \psi_2}{\partial n} - \psi_2 \frac{\partial \psi_1}{\partial n} \right] dl. \quad (43)$$

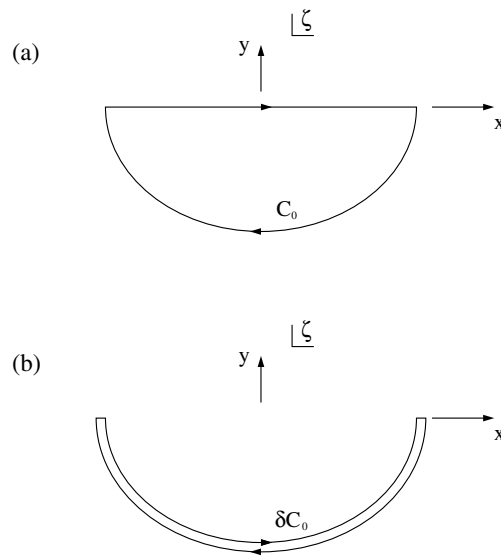


Figure 2. (a) Initial crack domain showing the enclosing path C_0 . (b) Crack variation showing its enclosing contour δC_0 .

Assuming ψ_1 and ψ_2 satisfy the Laplace equation, the left-hand side vanishes. Noting that both $\delta\psi$ and $\psi + \delta\psi$ are Laplacian, the theorem can be used to show that the integral whose path, C_0 , encloses the original crack domain also vanishes. Consequently,

$$\delta Z = \beta \oint_{\delta C_0} \left[\delta\psi \frac{\partial(\psi + \delta\psi)}{\partial n} - (\psi + \delta\psi) \frac{\partial\delta\psi}{\partial n} \right] dl = \beta \int_{C_c} \delta\psi \frac{\partial\psi}{\partial n} dl = \beta \int_{C_c} \left(\frac{\partial\psi}{\partial n} \right)^2 \delta n dl, \quad (44)$$

where it has been noted once more that $\delta\psi$ and $\psi + \delta\psi$ vanish at the edge of the varied crack. By comparing (44) with (34) it can be seen that

$$\nabla_v Z(l) = \beta \left(\frac{\partial\psi}{\partial n} \right)^2 = \beta H_t^2(l), \quad (45)$$

where $H_t(l)$ is the tangential magnetic field at the edge of the crack.

6. Edge field evaluation

The normal derivative of the potential, $\partial\psi/\partial n$, required for the evaluation of the impedance gradient via equation (45), is evaluated as the sum of two parts:

$$\frac{\partial\psi}{\partial n} = \frac{\partial\psi_1}{\partial n} + \frac{\partial\psi_2}{\partial n}, \quad (46)$$

where ψ_1 is the rectangular crack solution, equation (15), and ψ_2 is found by mapping to the τ -domain to give a solution defined by equation (25). The terms in the right-hand side of equation (46) have been separately expanded and are given in explicit form below.

The normal derivation of ψ_1 is expressed as

$$\frac{\partial\psi_1}{\partial n} = \frac{\partial\psi_1}{\partial x} \frac{\partial x}{\partial n} + \frac{\partial\psi_1}{\partial y} \frac{\partial y}{\partial n} = \left[\frac{\partial\psi_1}{\partial x} \frac{\partial x}{\partial \eta} + \frac{\partial\psi_1}{\partial y} \frac{\partial y}{\partial \eta} \right] \frac{\partial \eta}{\partial n}, \quad (47)$$

where the derivatives of ψ_1 with respect to x and y are obtained simply from (15). From (20) and (21)

$$\left(\frac{\partial x}{\partial \eta}\right)_{\eta=\alpha} = \pi \sum_{\nu} \nu b_{\nu} \cos[\pi \nu(1 - \xi)] \quad (48)$$

and

$$\left(\frac{\partial y}{\partial \eta}\right)_{\eta=\alpha} = \pi \sum_{\nu} \nu a_{\nu} \sin[\pi \nu(1 - \xi)]. \quad (49)$$

Also

$$\frac{\partial \eta}{\partial n} = \left[\left(\frac{\partial x}{\partial \eta}\right)^2 + \left(\frac{\partial y}{\partial \eta}\right)^2 \right]^{-1/2}. \quad (50)$$

From (24) and the fact that $\partial \phi / \partial \xi$ is zero at the corresponding boundary, the normal derivative of ψ_2 at the crack edge is written as

$$\frac{\partial \psi_2}{\partial n} = \left(\frac{\partial \phi}{\partial \eta}\right) \left(\frac{\partial \eta}{\partial n}\right) \quad (51)$$

where, from (25),

$$\left(\frac{\partial \phi}{\partial \eta}\right)_{\eta=\alpha} = \sum_n C_n n \pi \cos(n \pi \xi) \tanh(n \pi \alpha). \quad (52)$$

The relationships summarized in this section are used to evaluate the function gradient of the impedance, equation (45), in terms of the solution of the direct problem and a general mapping.

7. Parameter search

From (44), the derivative of the impedance with respect to parameter p_j is given by

$$\frac{\partial Z}{\partial p_j} = \beta \int_0^1 \left\{ \frac{\partial \psi}{\partial n} \right\}^2 \left[\frac{\partial n}{\partial p_j} \right] \left[\frac{\partial l}{\partial \xi} \right]_{\eta=\alpha} d\xi, \quad (53)$$

with

$$\left[\frac{\partial n}{\partial p_j} \right] \left[\frac{\partial l}{\partial \xi} \right]_{\eta=\alpha} = \left[\frac{\partial y}{\partial p_j} \right] \left[\frac{\partial x}{\partial \xi} \right]_{\eta=\alpha} - \left[\frac{\partial x}{\partial p_j} \right] \left[\frac{\partial y}{\partial \xi} \right]_{\eta=\alpha}. \quad (54)$$

For example, suppose the crack is assumed to be semi-elliptical with the shape represented by the parametric equations

$$x = x_0 + a \cos[\pi(1 - \xi)] \quad (55)$$

and

$$y = b \sin[\pi(1 - \xi)]. \quad (56)$$

The parameters a , b , and x_0 are sought where x_0 is the coordinate of the mid-point of the line joining the foci of the ellipse. Then, noting that $\partial x / \partial a = \cos[\pi(1 - \xi)]$ and $\partial y / \partial a = 0$, it is found that

$$\left[\frac{\partial n}{\partial a} \right]_l \left[\frac{\partial l}{\partial \xi} \right]_{\eta=\alpha} = \pi b \cos^2[\pi(1 - \xi)]. \quad (57)$$

Similarly,

$$\left[\frac{\partial n}{\partial b} \right]_l \left[\frac{\partial l}{\partial \xi} \right]_{\eta=\alpha} = \pi a \sin^2[\pi(1 - \xi)] \quad (58)$$

Table 1. Coil parameters.

Parameter	Value
Outer radius	7.50 ± 0.05 mm
Inner radius	2.51 ± 0.01 mm
Axial length	4.99 ± 0.01 mm
Nominal lift-off	0.10 ± 0.01 mm
Number of turns	4000 ± 1

and

$$\left[\frac{\partial n}{\partial x_0} \right]_l \left[\frac{\partial l}{\partial \xi} \right]_{\eta=\alpha} = \pi b \cos[\pi(1 - \xi)]. \quad (59)$$

Hence, with (53), the impedance derivative can be found for carrying out a search for semi-elliptical crack parameters. In dealing with an epicyclic crack with elliptical components such as shown in figure 1, the required derivatives are computed from the following relationships:

$$\left[\frac{\partial n}{\partial x_0} \right]_l \left[\frac{\partial l}{\partial \xi} \right]_{\eta=\alpha} = \pi \sum_{\nu} b_{\nu} \cos[\nu\pi(1 - \xi)], \quad (60)$$

$$\left[\frac{\partial n}{\partial \alpha} \right]_l \left[\frac{\partial l}{\partial \xi} \right]_{\eta=\alpha} = \left\{ \pi \sum_{\nu} \nu a_{\nu} \sin[\nu\pi(1 - \xi)] \right\}^2 + \left\{ \pi \sum_{\nu} \nu b_{\nu} \cos[\nu\pi(1 - \xi)] \right\}^2 \quad (61)$$

and

$$\begin{aligned} \left[\frac{\partial n}{\partial K_m} \right]_l \left[\frac{\partial l}{\partial \xi} \right]_{\eta=\alpha} &= \pi \sinh(\pi m \alpha) \sin[m\pi(1 - \xi)] \sum_{\nu} \nu a_{\nu} \sin[\nu\pi(1 - \xi)] \\ &+ \pi \cosh(\pi m \alpha) \cos[m\pi(1 - \xi)] \sum_{\nu} \nu b_{\nu} \cos[\nu\pi(1 - \xi)]. \end{aligned} \quad (62)$$

In the initial phase of the calculation, the parameters a , b and x_0 are sought, treating the crack as a semi-ellipse. Further degrees of freedom are added later by including extra terms in the series representation of the crack profile. A term is added when the calculation has reached a point at which reduction in the cost function with each iteration is small and yet its value indicates that further reduction is possible.

8. Results

Impedance measurements by Harrison *et al* [13] on simulated cracks in the form of slots in aluminium plates have been used to test the parametric inversion scheme. Experimental data have been provided by these authors at 16 frequencies from 250 Hz upwards but because the present theory uses thin-skin approximations, the inversions are carried out using data at the highest frequency only, 50 kHz. The experimental data have previously been used to validate and test the accuracy of solutions of the thin-skin forward problem [11].

Four simulated cracks, designated D1, D2, D3 and D4, have been reconstructed assuming that the crack lies in a known plane and the crack opening c is also known. A parametric search could include the crack opening but at present it is held fixed while the profile is sought. Predefined coil parameters and specimen parameters are given in tables 1 and 2.

For the first iteration, the search is restricted to fit a semi-ellipse by adjusting the location of the crack centre, the semi-major axis and the semi-minor axis. When the cost function is no longer decreasing with each iteration, an addition term is added to the parametric representation of the crack. This process continues until the cost function cannot be reduced by adding more

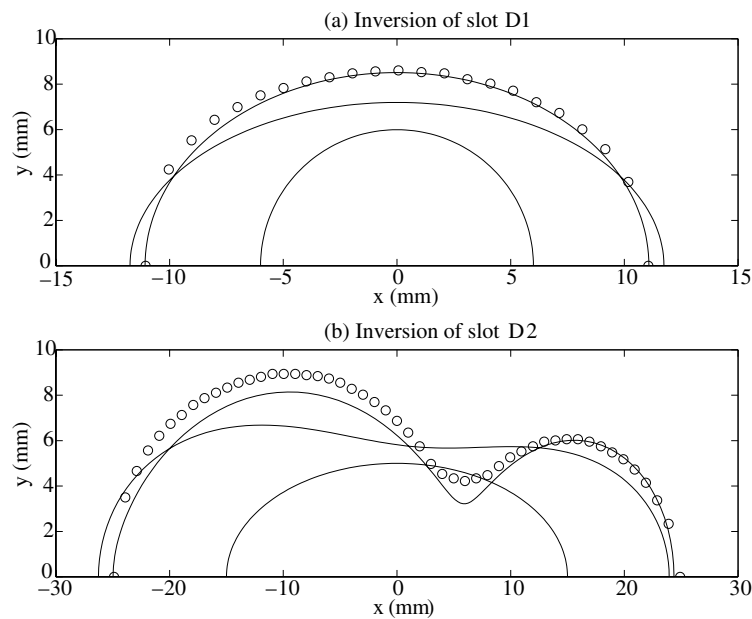


Figure 3. (a) Parametric reconstruction of slot D1 showing the profile at iterations 1, 3 and 5, solid curves. (b) Parametric reconstruction of slot D2 showing iterations 1, 25 and 35. Measured profile data are shown as circles.

Table 2. Slot parameters and coil lift-off.

Parameter	Slot D1	Slot D2	Slot D3	Slot D4
Max opening (mm)	0.33 ± 0.01	0.37 ± 0.01	0.32 ± 0.01	0.30 ± 0.01
Conductivity (MS m^{-1})	22.50 ± 0.05	22.40 ± 0.05	23.15 ± 0.05	23.20 ± 0.05
Coil lift-off (mm)	0.491 ± 0.01	0.318 ± 0.01	0.368 ± 0.01	0.498 ± 0.01

Table 3. Inversion results.

Parameter	Slot D1	Slot D2	Slot D3	Slot D4
No of measurements used	11	19	11	19
Measurement step (mm)	4	4	4	4
Length measured (mm)	22.10 ± 0.05	49.78 ± 0.05	24.84 ± 0.05	48.41 ± 0.05
Length by inversion (mm)	22.16 ± 0.50	49.34 ± 0.50	25.21 ± 0.50	48.78 ± 0.50
Max. depth measured (mm)	8.61 ± 0.05	8.94 ± 0.05	9.04 ± 0.05	8.36 ± 0.05
Max. depth inversion (mm)	8.51 ± 0.80	8.15 ± 0.80	8.72 ± 0.80	8.16 ± 0.80

degrees of freedom in the representation of the crack shape. At this point the algorithm is terminated. For flaws D1 and D3, the algorithm terminates with three terms in the series expansions, equations (20) and (21). For flaws D2 and D4, five terms are needed.

The results of a parameter search for the shape of D1 and D2 are illustrated in figure 3. Similar results for D3 and D4 are shown in figure 4. Table 3 compares the length and depth of the slots found by inversion with the values found by direct measurement.

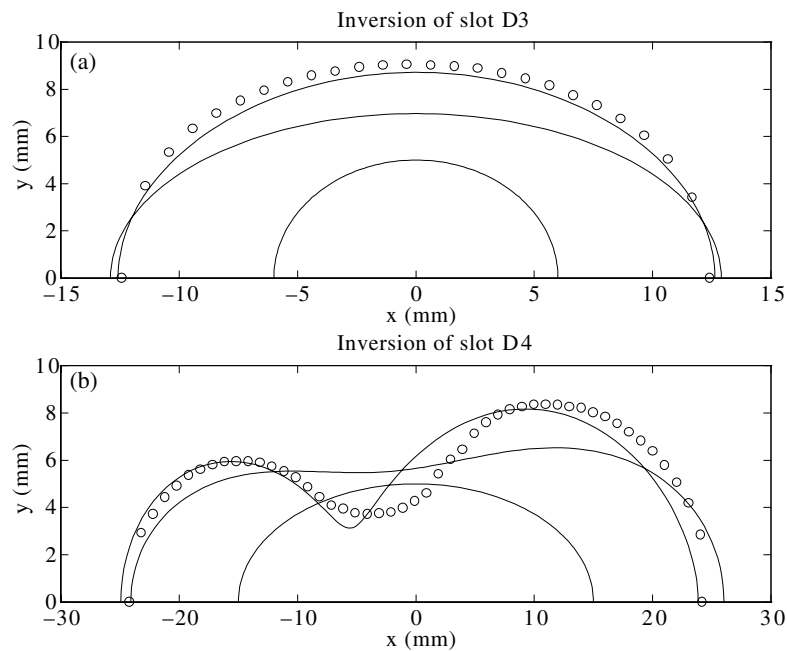


Figure 4. (a) Parametric reconstruction of slot D3 showing the profile at iterations 1, 10 and 11 as solid curves. (b) Parametric reconstruction of slot D4 showing iterations 1, 25 and 35. Measured profile data are shown as circles.

9. Conclusion

In an optimization approach to inversion, the central task is to find a means of updating the flaw in such a way that the agreement between theoretical predictions and observations is improved. For a number of cases [14], this update has been expressed in terms of the gradient of the observations with respect to a variation of the flaw using the adjoint method. In earlier work, the approach was used to perform inversion calculations using a forward model in which the effect of an ideal closed crack is represented in terms of a surface current dipole distribution [3]. The dipole density is determined using a boundary element scheme and the probe impedance changes due to the crack calculated from a numerical approximation of the dipole density. This model is valid at low frequencies where the skin depth is much greater than the crack opening. At higher frequencies it is possible to account for the effect of the opening in a simple way by approximating the electric field inside the crack as normal to the crack faces and adapting the boundary element calculation accordingly [15]. The boundary element schemes seem to be more efficient at low and intermediate frequencies, but at high frequencies a large number of elements is needed and the computation cost is high. This cost has been avoided in this study by using an alternative approach based on thin-skin approximations. The functional gradient of the impedance with respect to a variation of the line of the crack edge has now been determined for thin-skin crack profile inversion. The gradient is expressed simply in terms of the magnetic field tangential to the crack edge.

As alternatives to (32), other cost functions can be defined which use only the resistive or the inductive component of the observations. There may be advantages in doing this if one or other component is more accurately measured, or is in better agreement with the prediction of

the forward problem. In either case, the gradient of the new cost function can be expressed in terms of the functional gradient of the impedance with respect to a variation of the crack profile. Hence the method presented here is easily adapted to deal with different cost functions by making minor modifications to the function definition (32) and the gradient (36).

In testing the inversion scheme using impedance measurements of a normal coil on simulated cracks, the profiles found by inversion were in good agreement with the measured shapes. It must be acknowledged that in industrial conditions, the signal-to-noise ratio of the data is not usually as high as that of the experimental results used in this work. In addition, the ultimate applications must deal with fatigue cracks that can be irregular, subject to stress fields and may have points of electrical contact between faces. All of these factors will reduce the accuracy of the inversion. However, the preliminary steps taken in this study have shown that without presupposing the slot shapes the lengths can be determined from eddy current data to within 3% and the depths to within 10%.

References

- [1] Mester M L and McIntire P (ed) 1986 *Nondestructive Testing Handbook* vol 4 *Electromagnetic Testing* 2nd edn (Columbus, OH: ASNT Publications)
- [2] Bowler J R 1994 Eddy-current interaction with an ideal crack: I. The forward problem *J. Appl. Phys.* **75** 8128–37
- [3] Bowler J R, Norton S J and Harrison D J 1994 Eddy-current interaction with an ideal crack: II. The inverse problem *J. Appl. Phys.* **75** 8138–44
- [4] Kahn A H, Spal R and Feldman A 1977 Eddy-current losses due to surface crack in conducting material *J. Appl. Phys.* **48** 4454–9
- [5] Sommerfeld A 1964 *Optics* (New York: Academic)
- [6] Harfield N and Bowler J R 1994 Analysis of eddy-current interaction with a surface-breaking crack *J. Appl. Phys.* **76** 4853–6
- [7] Auld B A, Jefferies S R and Moulder J C 1988 Eddy-current signal analysis and inversion for semielliptical surface cracks *J. Nondestruct. Eval.* **7** 79–94
- [8] Burke S K 1994 Eddy-current inversion in the thin skin limit: determination of depth and opening of a long crack *J. Appl. Phys.* **76** 3072–80
- [9] Harfield N and Bowler J R 1997 Theory of thin-skin eddy-current interaction with surface cracks *J. Appl. Phys.* **82** 4590–603
- [10] Bowler J R and Harfield N 1998 Evaluation of probe impedance due to thin-skin eddy-current interaction with surface cracks *IEEE Trans. Magn.* **34** 515–23
- [11] Bowler J R and Harfield N 2000 Thin-skin eddy-current interaction with semi-elliptical and epi-cyclic cracks *IEEE Trans. Magn.* **36** 281–91
- [12] Dodd C V and Deeds W E 1968 Analytical solutions to eddy-current probe-coil problems *J. Appl. Phys.* **39** 2829–38
- [13] Harrison D J, Jones L D and Burke S K 1996 Benchmark problems for defect size and shape determination in eddy-current nondestructive evaluation *J. Nondestruct. Eval.* **15** 21–34
- [14] Norton S J and Bowler J R 1992 Theory of eddy-current inversion *J. Appl. Phys.* **73** 501–12
- [15] Bowler J R 2000 Inversion of open cracks using eddy current probe impedance measurements *Review of Progress in Quantitative Nondestructive Evaluation* ed D O Thompson and D E Chimenti (New York: Plenum) pp 529–33